HHS Public Access

Author manuscript

Nat Neurosci. Author manuscript; available in PMC 2009 May 01.

Published in final edited form as:

Nat Neurosci. 2008 November ; 11(11): 1343–1351. doi:10.1038/nn.2199.

Origin of correlated activity between parasol retinal ganglion cells

Philipp Khuc-Trong and **Fred Rieke**

Howard Hughes Medical Institute Department of Physiology and Biophysics University of Washington Seattle, WA 98195

Abstract

Cells throughout the central nervous system exhibit synchronous activity patterns - i.e. a cell's probability of generating an action potential depends both on its firing rate and on the occurrence of action potentials in surrounding cells. The mechanisms producing synchronous or correlated activity are poorly understood despite its prevalence and potential impact on neural coding. We find that neighboring parasol retinal ganglion cells receive strongly correlated synaptic input in the absence of modulated light stimuli. This correlated variability appeared to arise through the same circuits that provide uncorrelated synaptic input. In addition, ON but not OFF parasol cells were coupled electrically. Correlated variability in synaptic input, however, dominated correlations in the parasol spike outputs and shared variability in the timing of action potentials generated by neighboring cells. These results provide a mechanistic picture of how correlated activity is produced in a population of neurons of key importance to visual perception.

INTRODUCTION

Correlated or synchronous activity challenges our mechanistic understanding of how signals propagate through neural circuits and our functional interpretation of how they are encoded by neural populations (reviewed in refs. 1,2). Functionally, correlated activity could convey information that is inaccessible when neural responses are considered one at a time3-5 or could permit elimination of common noise from population responses6. Alternatively, correlated activity could represent redundancy or inefficiency in the coding of input signals, and as such limit the benefits of averaging responses over multiple cells7-9. These functional extremes (see also ref. 10) suggest corresponding differences in the underlying mechanisms. Few studies, however, directly investigate the mechanistic basis of correlated activity under physiological conditions.

Nearby retinal ganglion cells exhibit correlated activity in the absence of modulated light stimuli (reviewed in refs. 11-13). This stimulus-independent correlated activity must be produced by statistical variations in photon arrival and/or by spontaneous activity within retinal circuits. Synchronous activity patterns can extend to include many ganglion cells14.

Correspondence: Fred Rieke HHMI/Department of Physiology & Biophysics University of Washington 1959 NE Pacific Street, HSB J187 Seattle, WA 98195-7290 206-616-6956 (phone) 206-221-3946 (fax) rieke@u.washington.edu.

These larger synchronous events do not necessarily require direct connections among all participating cells but instead could be produced by interactions among smaller groups of cells. Indeed, correlations between pairs of nearby ganglion cells appear to explain much of the synchronous activity generated in the entire population15,16. This focuses work investigating the mechanisms mediating synchronous activity on interactions between pairs of cells.

Shared synaptic input and/or reciprocal synaptic connections could mediate correlated activity in the retina and other neural circuits. Anatomical and physiological studies provide evidence for both shared input and reciprocal electrical coupling in retina17-26. However, uniquely identifying the contribution of these two mechanisms to correlated activity and more broadly to neural coding has been difficult because of (1) significant species differences, (2) heterogeneity in the strength of correlations among different ganglion cell types, and (3) a lack of intracellular recordings from the cells involved (exceptions are refs. 25,26). Understanding how the mechanisms producing correlated activity relate to visual function will require a complete mechanistic picture for correlated activity in a population of identified ganglion cells.

Here we use paired patch-clamp recordings to investigate the basis of correlated activity between parasol ganglion cells in primate retina. These cells play a key role in visual function since they provide the dominant input to dorsal stream visual processing areas. A wealth of anatomical information about the circuitry providing input to parasol cells provides an important tool for understanding how correlations are produced (reviewed in ref. 27). Further, primate retina offers a unique opportunity to relate mechanistic studies of correlated activity to existing information about synchronous activity and neural coding in populations of identified ganglion cells5,16,28.

RESULTS

Common noise in the input to neighboring parasol cells

We isolated correlations in excitatory and inhibitory synaptic inputs to neighboring parasol cells using paired voltage-clamp recordings; these conditions should suppress reciprocal coupling via gap junctions, which depends on the voltage difference between the two cells. We start with excitatory inputs, which are more likely to produce rapid correlations in action potential generation.

Correlated variability in excitatory synaptic inputs during constant light— Simultaneously recorded excitatory synaptic inputs to pairs of ON (Fig. 1a) and pairs of OFF (Fig. 1b) parasol cells exhibited clear correlations (Fig. 1c and d). These correlations were present without modulated light input, as in Fig. 1, and thus represent noise within the retinal circuitry that produces correlated variability in the synaptic inputs to the cells (‘common noise’ for short). As described below, correlated and uncorrelated input appeared to originate through the same circuitry.

Substantial differences in the kinetics of correlated and uncorrelated input would indicate distinct circuit origins. Thus we compared the cross-correlation function with the

autocorrelation function corrected for the contribution from common noise (Fig. 1c and d, right; see Methods for details). We emphasized ON pairs because of their stronger common noise. The widths of the cross-correlation and corrected autocorrelation were similar; the full width at half maximum was 9 ± 1 ms (mean ± SEM, n=16) for the cross-correlation and 7 ± 1 ms for the corrected autocorrelation. The characteristic oscillatory shape of both correlation functions (Fig. 1c) indicates that synaptic input to a single cell and common noise in the input to neighboring cells were anticorrelated for time shifts of 10-20 ms. These similarities in the kinetics of correlated and uncorrelated excitatory synaptic input are consistent with a common origin.

The dependence of common noise on dendritic overlap also constrains its origin. For example, common noise could be produced if neighboring ganglion cells sense glutamate release from a single presynaptic vesicle release site. Such a model predicts that common noise is present only when the dendrites of the two cells are within 1-2 μm - an upper bound on how far glutamate can diffuse before uptake. This prediction failed. We quantified dendritic overlap from cumulative distributions of nearest-neighbor distances between dendrites of the two cells (Figs. 1e-g; see Methods). For the cell pair in Figure 1e, < 2% of the locations on the dendrites of one cell were within 2 μm of a location on the neighboring cell's dendritic tree (Fig. 1g, thick trace). Nonetheless this cell pair had a peak cross-correlation of 0.14 (Fig. 1h). The peak cross-correlation characterizes the fraction of the total variance in excitatory synaptic input shared by the two cells. In the simplest scenario, inputs are distributed uniformly across the dendrites and summed linearly. In this case, the fraction of dendritic overlap predicts the fraction of shared variance, so 2% dendritic overlap would correspond to a cross-correlation peak of 0.02. Another cell pair with less overlap showed even stronger common noise (Fig. 1h). The persistence of common noise in cells with few opportunities to sample common vesicle release sites indicates that it is produced by coordinated release at distinct sites.

The opposite extreme of that considered above is that common noise is a consequence of a wide field amacrine cell that provides direct excitatory input to both ganglion cells or coordinates release from multiple bipolar synapses. Common noise produced by a source with a spatial extent large compared to the ganglion cell dendrites should be insensitive to dendritic proximity. This prediction again failed: cell pairs with more dendritic overlap exhibited stronger common noise (Fig. 1h; $p < 0.05$). Defining dendritic overlap by the fraction of nearest-neighbor locations within 17 μm (as in Fig. 1h) equated the average overlap with the average peak cross-correlation across ON cell pairs; definitions of overlap based on nearest-neighbor distances less than 10 μm or greater than 25 μm caused overlap and correlation strength to differ systematically (Supplementary Fig. 1 online). Thus the dependence of common noise on dendritic overlap is consistent with synaptic input from a presynaptic element 10-25 μm in extent - e.g. the axon terminals of the DB4 and DB5 diffuse cone bipolar cells that make synapses onto the parasol dendrites29.

In sum, the experiments of Figure 1 indicate that neighboring ON parasol cells receive strongly correlated excitatory inputs, with ∼25% of the total variance in the input shared (Fig. 1c, right). The kinetic and spatial properties of this common noise suggest that it originates from the same circuitry that provides uncorrelated input (see Discussion).

Neighboring OFF parasol cells receive weaker correlated excitatory input during constant light.

Differences in the excitatory inputs to ON and OFF parasol cells—The weaker common noise in the excitatory synaptic inputs to OFF parasol cells could reflect differences in retinal circuitry or differences in the functional response properties of ON and OFF parasol cells. In particular, synaptic nonlinearities could obscure correlations arising earlier in the circuitry, just as the nonlinearity of spike generation can confound estimates of correlated input based on observations of correlated action potentials30. Indeed, as shown below, the excitatory synaptic inputs of OFF parasol cells exhibited substantially stronger nonlinearities than those of ON parasol cells.

In constant light the excitatory synaptic input to OFF (Fig. 2b) but not ON (Fig. 2a) parasol cells lingered near the minimal value reached during the modulated light (dashed line). ON cells received substantially more tonic excitatory synaptic input than OFF cells (Fig. 2d; $p < 10^{-12}$). Correspondingly, distributions of current amplitudes of OFF parasol cells (Fig. 2e) showed a greater probability of small values than those of ON parasol cells (Fig. 2c). Similar differences have been observed in guinea pig alpha ganglion cells31. As described below, this difference is an important determinant of the strength of correlated input that neighboring cells receive.

Modulated light stimuli alter common noise in neighboring OFF but not ON parasol cells—Is common noise in the excitatory synaptic input to neighboring parasol cells altered by modulated light stimuli? As described below, common noise in OFF parasol cells was stronger in the presence of modulated light compared to constant light, while common noise in ON parasol cells was insensitive to changes in light input.

Figures 3a and b show sections of the current responses to a time-varying stimulus (top trace) for the same pairs as Figure 1. To compare the fluctuations present during constant light with the fluctuations about the mean response to the modulated light stimulus, we subtracted the average response to repeated stimulus presentations from each individual response. For ON parasol cells, the resulting residuals and the noise in synaptic input during constant light were similar (Fig. 3c); for OFF parasol cells, the two were quite different (Fig. 3d).

The residuals of the responses to the time-varying stimulus, like the responses during constant light, exhibited clear correlations. However, the stimulus-dependence of the correlated variability in excitatory synaptic input differed between ON and OFF parasol cells. The left panels in Figures 3e and f compare cross-correlation functions measured under three conditions: (1) for the full responses to the time-varying stimulus (blue); (2) for the residuals of the responses to the time-varying stimulus (red); and (3) for the responses in constant light (black). Across ON parasol pairs, the cross-correlation function for the residuals closely matched that for constant light (Fig. 3e, right). Thus, for ON pairs, correlated noise accounted for a similar fraction of the variance in total synaptic input during constant light and during stimuli that strongly modulated synaptic input. For OFF parasol

pairs the correlations were stronger in the presence of modulated light (Fig. 3f, right; $p < 0.001$).

The weaker common noise of OFF parasol cells in constant light (Fig. 1c and d) and greater dependence of correlation strength on modulated light stimuli (Fig. 3e and f) are consistent with the smaller tonic excitatory synaptic input OFF parasol cells receive during constant light (Fig. 2). With little tonic input, noise intrinsic to the ganglion cell could contribute more to the total variance and hence obscure correlations in the input currents. Time-varying stimuli produce large synaptic inputs, which could reveal correlated input. Indeed, the correlations in excitatory synaptic inputs to OFF parasol pairs in the presence of modulated light were similar in magnitude to those of ON parasol pairs.

In principle, common noise could originate from activation of the cone photopigment (due to either spontaneous activation or Poisson fluctuations in photon absorption). However, the cross-correlation functions for both residuals and constant light responses were narrower than those for the full responses to time-varying stimuli (left panels in Fig. 3e and f). The rapid kinetics of common noise are inconsistent with an origin in the cone photopigment, which should produce correlations with a time scale similar to that of the responses to rapidly fluctuating light stimuli.

Correlated variability in inhibitory synaptic inputs—Inhibitory synaptic inputs alone are not likely to produce rapid (< 10 ms) correlations in the spike outputs of neighboring ganglion cells, but they could shape such correlations. Thus we repeated the experiments of Figures 1 and 3 while isolating inhibitory synaptic inputs to neighboring parasol cells. Figure 4 summarizes the results, in the same format as Figure 3. Both ON and OFF parasol cells received abundant inhibitory input in the presence of a modulated light stimulus (Fig. 4a, b). In both cell types, residuals of the responses to the modulated stimulus were more strongly correlated than currents measured during constant light (right panels in Fig. 4e, f). Inhibitory inputs were more weakly correlated than excitatory inputs in ON cells, while in OFF cells correlations in excitatory and inhibitory inputs had similar strength.

ON but not OFF parasol cells show effective reciprocal connections

The experiments described above characterize common noise in the synaptic inputs to neighboring parasol cells. Common noise alone, however, did not appear sufficient to explain the correlation between the spike outputs of neighboring ON cells. In particular, the cross-correlation function for the spike responses of neighboring ON parasol cells typically exhibited two peaks, separated by ∼2 ms (e.g. Fig. 6b). Similar two-peaked cross-correlation functions in other species have been attributed to electrical synapses that mediate reciprocal - or at least effectively reciprocal - connections between the two cells[21,23-25]. The separation between the peaks presumably reflects the time required for signals to propagate from one cell to the other. The experiments described below show that neighboring ON but not OFF parasol cells are coupled electrically.

Stepping the voltage of one ON parasol cell produced a current in a neighboring ON parasol cell (Fig. 5a) that scaled near linearly with the voltage step (Fig. 5c and d). The coupling was also effectively reciprocal; similar current changes were produced by stepping the

voltage of either cell while monitoring current in the other (Fig. 5c). These experiments were all performed with receptors mediating chemical synaptic transmission blocked, which decreased the noise in the ON parasol cell currents by a factor of ∼50. In a few cell pairs coupling was apparent when chemical synaptic transmission was operational, but in most cases it was obscured by synaptic noise. The strength of coupling did not differ noticeably when it was measured in the presence and absence of chemical synaptic transmission.

Effective reciprocal coupling between neighboring ON parasol cells did not require extensive dendritic overlap. For example, the ON parasol pair shown in Figure 1e exhibited clear coupling, although the direct contact between dendrites was minimal (< 2% of the dendrites were within 2 μm). The persistence of reciprocal connections in cells with little dendritic overlap is consistent with tracer injection studies that suggest that electrical coupling between parasol cells is mediated through an amacrine cell18,22.

OFF parasol cells did not exhibit measurable coupling (Fig. 5b, d and e) in the presence or absence of chemical synaptic transmission. The coupling resistance between OFF parasol cells was at least 100 times higher than that between ON parasol cells (Fig. 5d). OFF parasol pairs lacking measurable coupling often had substantial dendritic overlap.

Contributions of common noise and reciprocal connections

Impact of common noise and reciprocal connections on spike train correlations—

What contributions do common noise and reciprocal connections make to correlations in the spike outputs of neighboring ON parasol cells? Direct experimental approaches to this question using currently available pharmacology (e.g. attempting to block gap junctions) would be difficult to interpret because of the possibility of unanticipated effects on other components of the retinal circuitry. Thus we generated a model that allowed us to vary the strength of common input and reciprocal connections while monitoring correlations in the predicted spike trains (Fig. 6a; see Methods). The model focused on correlations in excitatory synaptic inputs since they were ∼5x stronger than those in inhibitory inputs.

Each ganglion cell received uncorrelated and correlated synaptic input approximating the inputs ON parasol cells receive during constant light (Fig. 1c, right). The kinetics of the uncorrelated input were determined by the corrected autocorrelation function for excitatory synaptic input to a cell. Similarly, the kinetics of the correlated input was determined by the measured cross-correlation function. These two sources of synaptic input were scaled and summed so that correlated input accounted for 30% of the total current variance (see Fig. 1c). Currents were converted to voltages by filtering with an RC filter that approximated the measured properties of the cell membrane. A stereotyped (measured) action potential replaced the subthreshold voltage waveform each time the voltage crossed threshold with a positive derivative. Absolute and relative refractory periods followed each action potential. The voltage difference between the two cells (including action potentials) and the measured coupling resistance (Fig. 5d) determined the coupling current.

The model aimed to replicate the strength and shape of the measured cross-correlation functions for ON parasol spike responses during exposure to constant light (e.g. Fig. 6b).

With all parameters set equal to the mean experimental values (with no free parameters; see Methods), the model captured the magnitude of the typical experimental cross-correlation function and the splitting of the peaks (Fig. 6c). Reciprocal connections alone produced much weaker correlations than observed (Fig. 6d), while common synaptic input alone more closely captured the overall strength of the correlations but not the splitting of the peaks (Fig. 6e).

Across the range of experimentally observed values for the coupling resistance (640 MΩ to 1.5 GΩ), reciprocal connections accounted for < 25% of the area of the central peak of the cross-correlation function. Only when the coupling resistance was decreased to one quarter of the measured value did reciprocal connections and common noise make similar contributions to the strength of correlated activity. Changes in other model parameters (see Methods) influenced the separation between the two peaks in the predicted cross-correlation function, but had little effect on the relative importance of common noise and reciprocal connections to the overall strength of correlated activity. Thus across a broad parameter range common noise dominated the strength of correlations between neighboring ON parasol cells, although reciprocal connections were required to explain the two-peaked correlation functions.

Correlations produce common jitter in light-evoked spike trains—Several sources of noise contribute to variability in a ganglion cell's output spike trains. Some of these - e.g. noise in the spike generation process itself - will be independent in neighboring ganglion cells while others - e.g. common noise in synaptic inputs - will be shared. We used a spike distance metric32 to determine to what extent the combination of common noise and reciprocal connections produced shared variations in spike timing in neighboring cells.

The spike distance metric compares two spike trains by converting one into the other through three basic operations: (1) deleting spikes; (2) adding spikes; and (3) shifting spikes in time. Given the relative distances associated with each operation, the metric identifies the unique set of operations that minimizes the total distance between the two spike responses. Under conditions where shifting a spike ≤ 20 ms incurred less distance than deleting a spike, >70% of the spikes were matched via the shifting operation in comparisons of simultaneously measured spike trains from two neighboring cells. We quantified precision from the time differences between these spikes33.

Figure 7 shows cell-attached recordings of spike responses from neighboring ON (Fig. 7a) and OFF (Fig. 7b) parasol cells to two repetitions of the same modulated stimulus. We used the spike distance metric to compare: (1) responses of two cells on the same stimulus trial (red); (2) responses of the two cells on different stimulus trials (black); and (3) responses of each individual cell on different trials (blue). Figures 7c and e plot the cumulative distribution of time differences ΔT between spikes matched via the shifting operation for each of these comparisons. An increase in temporal precision (smaller ΔTs) shifts the cumulative distribution to the left. All comparisons of nonsimultaneous spike trains revealed similar temporal precision, whether the comparison was made between two responses of the same cell (blue circles) or one response from each cell (black line). Thus systematic differences in sensitivity or timing between neighboring cells were relatively small.

Simultaneous spike trains in the two neighboring cells (red line) had the greatest precision, indicating that trial-to-trial variability in spike times was correlated in the two cells.

Median ΔTs for nonsimultaneous spike trains were consistently smaller than those for simultaneously recorded spike trains (Fig. 7d). The relatively modest (∼30%) shift in precision is expected since the minority of the variance in the synaptic input to a cell was shared with a neighboring cell while the majority of the input variance was uncorrelated.

In the presence of modulated light inputs, the strength of the common noise in the inputs to pairs of ON and OFF parasol cells was similar, while only ON parasol pairs showed reciprocal connections. Thus, if reciprocal connections dominate correlated variability in spike times between neighboring cells, the common jitter in spike timing of ON cells should be greater than that of OFF cells. Contrary to this prediction, the difference in median ΔT between simultaneous and nonsimultaneous responses was similar for ON and OFF pairs (Figure 7d). Thus common variability in synaptic input rather than reciprocal connections appears to dominate the common jitter in the spike responses of neighboring ON and OFF parasol cells.

DISCUSSION

Despite the prevalence of correlated activity in the nervous system, we have a primitive understanding of the mechanisms responsible and their relation to neural coding. Here we explored the mechanistic origin of correlated activity between neighboring parasol cells in primate retina; the picture this work provides complements recent work on the functional significance of correlated activity in the same cells5,16. We reached three main conclusions. First, pairs of both ON and OFF parasol cells receive strongly correlated synaptic input, likely through the same circuits that provide uncorrelated input. Second, ON but not OFF parasol cells are coupled reciprocally. Third, common noise dominates the strength of correlations in the action potentials generated by neighboring cells and the shared variability in action potential timing. Figure 8 illustrates a working model suggested by these results; below we elaborate each aspect of the model and the possible implications for neural coding.

Correlated variability in synaptic input to neighboring ganglion cells

Two distinct sources of common noise contribute to correlations between neighboring ganglion cells. Slow correlations (50-100 ms) have been attributed to shared photoreceptor noise20,23. In dark-adapted cat retina, neighboring ganglion cells generate correlated bursts of action potentials20. The rate of occurrence, duration and dependence on dim steady light all suggest these bursts are produced by spontaneous photon-like noise events generated in the rod photoreceptors. More rapid correlations (∼5 ms in mammalian retina) dominate correlated activity at higher light intensities. In salamander, block of chemical synaptic transmission eliminates slow but not fast correlations23. However, in mammalian retina ON and OFF ganglion cells can exhibit anticorrelated activity19, implying that chemical synaptic transmission is involved. The rapid kinetics of these correlations have been used to argue that they depend on a cell capable of generating action potentials - e.g. a spiking amacrine cell19,24. These considerations suggest that correlated input could be produced

through a different circuit than uncorrelated input. Indeed, amacrine cells make numerous synapses on the dendrites of parasol ganglion cells22,34,35.

The experiments described here add to and modify this picture. Correlated variability in the synaptic inputs to neighboring ganglion cells was measured directly rather than inferred from correlations in spike outputs. This common noise was strong, accounting for more than 25% of the variance in a cell's excitatory synaptic input. The kinetics of uncorrelated and correlated synaptic input were similar. Thus, the kinetics of the uncorrelated synaptic input were sufficiently fast that it was not necessary to posit a separate source of correlated synaptic input (e.g. from a spiking amacrine cell).

The dependence of common noise on dendritic overlap is consistent with a source of common input 10-25 μm in extent; substantially larger or smaller presynaptic elements predict stronger or weaker common noise given the measured dendritic overlap (Fig. 1h and Supplementary Fig. 1 online). In principle, an interneuron such as the AII amacrine cell could correlate signals in nearby bipolar cells. Such a mechanism, however, appears unlikely given the small apparent spatial extent of the source of common input. The DB4 and DB5 bipolar cells that contact ON parasol dendrites have axon terminals spanning ∼18-22 μm29. Thus coupling of signals in nearby bipolar cells would produce correlations with a spatial extent inconsistent with the measured dependence of correlation strength on dendritic overlap. The AII amacrine dendrites similarly span ∼45 μm36. These observations suggest that independent signals in the diffuse bipolar cells, which provide the majority of excitatory input to ganglion cells, provide common noise (Fig. 8). We discuss the functional implications of this conclusion below.

Reciprocal connections between nearby ganglion cells

The most rapid interactions between nearby ganglion cells, with a time scale ∼1 ms, are caused at least in part by electrical interactions between neighboring cells. Three types of experiment support this view. First, eliciting an action potential in one cell can increase the firing probability in a nearby cell21,25. Paired intracellular recordings in rat show reciprocal and symmetrical coupling, as expected for typical electrical synapses26. Second, cross-correlation functions often show two peaks, separated by 1-2 ms (e.g. Fig. 6b), suggesting reciprocal connections21,23,24. In salamander these rapid correlations are resistant to block of chemical synaptic transmission23. Third, tracer coupling and electron microscopy studies provide evidence for electrical synapses between ganglion cells26 and between ganglion and amacrine cells18,22. In rabbit, ganglion cells exhibiting rapid correlations are tracer coupled, whereas cells lacking correlations are not25.

The paired intracellular recordings described here provide direct evidence for effectively reciprocal connections via gap junctions between ON (but not OFF - see below) parasol cells. The ∼900 MΩ resistance of these electrical synapses is comparable to electrical synapses between cones37 and between AII amacrine cells38; however, the impact on signaling between parasol cells is likely much smaller than in these other cell types because the parasol input resistance is ∼10-fold less than that of cones or AII amacrine cells.

Relative contributions of common noise and reciprocal connections

We combined direct measurements of common noise and reciprocal connections to estimate their relative contributions to correlations in the spike output of neighboring ON parasol cells. We found that common noise accounted for the majority of the correlated activity, but reciprocal connections were required to explain the two-peaked structure apparent in the cross-correlation function (Fig. 6).

The model highlighted two other issues. First, the experimental coupling current produced by reciprocal connections depended on both subthreshold voltages and action potentials. Eliminating the dependence of coupling currents on subthreshold voltage had little impact on the predicted cross-correlation function. Thus, in the model, coupling currents produced by action potentials were primarily responsible for the two-peaked cross-correlation function, and, at least as far as correlated activity is concerned, the reciprocal connections can be approximated as being spike dependent. This will likely be an important simplification in larger scale models that aim to capture population dynamics (e.g. ref. 5).

Second, reciprocal connections alone were too weak to produce correlated action potentials. Reciprocal connections caused a spike in one cell to produce a ∼0.5 mV depolarization in a neighboring cell; this depolarization was considerably smaller than the ∼5 mV needed to reach spike threshold. Instead, reciprocal connections likely act to alter the occurrence and timing of spikes in the presence of correlated and uncorrelated synaptic inputs that depolarize a cell near threshold. Thus the contribution of reciprocal connections to correlated activity likely depends on the properties of the synaptic input the cells involved receive. This dependence will be an important factor in understanding the impact of reciprocal connections on coding of light inputs.

Functional asymmetries between ON and OFF cells

The standard description of ON and OFF retinal circuits is that they are antisymmetrical. A growing list of observations, however, refutes this picture: (1) dendritic and receptive field sizes of ON and OFF ganglion cells of the same type can differ systematically39-41; (2) responses of OFF parasol cells exhibit stronger nonlinearities than those of ON cells41; (3) the properties of excitatory and inhibitory synaptic inputs to ON and OFF cells can differ dramatically31,33; and (4) correlated activity between pairs of ON cells and pairs of OFF cells of the same type can differ24,25.

In rabbit retina, ON alpha ganglion cells exhibit a single peaked cross-correlation function, suggestive of common input, while OFF cells exhibit a two-peaked cross-correlation function24. Correspondingly, spikes elicited in an OFF (but not ON) alpha cell increased the firing probability in a neighboring cell25. Primate parasol ganglion cells show the opposite asymmetry: ON cells were coupled reciprocally, while OFF cells were not (Fig. 5; illustrated in Fig. 8). This asymmetry is unexpected from tracer coupling studies, which show coupling between both ON and OFF parasol ganglion cells18.

The properties of synaptic inputs to ON and OFF parasol cells also differed substantially. In particular, OFF parasol cells received much less tonic excitatory synaptic input during constant light than ON parasol cells (Fig. 2; Fig. 8 insets; see also ref. 31). This difference

likely contributes to (or explains) the greater nonlinearity in the spike outputs of OFF parasol cells41. Modulated light stimuli increased common noise in the synaptic inputs to neighboring OFF (but not ON) parasol cells. Thus nonlinearities within the neural circuits, like those in spike generation30, can obscure similarities in the mechanisms producing correlated or synchronous activity.

Implications of correlated activity for neural coding

The functional importance of correlated or synchronous activity is poorly understood in the retina and elsewhere in the central nervous system10,42 (reviewed in ref. 2). Thus synchronous activity could indicate redundancy, and a corresponding decrease in the capacity to convey information about sensory stimuli9; synchronous activity could carry a significant amount of information about sensory inputs5; or synchronous activity could be essentially irrelevant for how much information is encoded10.

The lack of a mechanistic understanding of how correlated activity is produced has hampered study of its functional importance. For example, correlations produced by reciprocal connections alone are likely to produce redundancy by causing the activity in one cell to replicate activity in a nearby cell. Common input, on the other hand, could produce a distributed or multiplexed code. A specific example of the latter is if synchronous activity is produced by common input from an interneuron with distinct temporal, chromatic or spatial sensitivity3,14. In this case, synchronous activity could convey a distinct message - that encoded by the response properties of the interneuron.

The finding that common input dominates the correlations between neighboring ON and OFF parasol cells supports the possibility of distributed coding. However, our results suggest that common input does not originate through a unique circuit but instead through a subset of the bipolar cells that make synaptic contacts with the parasol dendrites. In this case, correlated activity could serve to signal activity of these cells (see Figure 8). Such a picture suggests that correlated activity would primarily affect the encoding of spatial stimulus variations, consistent with work in salamander ganglion cells14. In general the picture that correlated activity is produced by dendritic overlap and corresponding shared bipolar synaptic input helps make specific and testable predictions about its functional impact.

METHODS

Tissue

Primate (*Macaca fascicularis*, *Macaca nemestrina*, and *Papio anubis*) retinas were obtained through the Tissue Distribution Program of the Regional Primate Research Center at the University of Washington and prepared as described previously43. All recordings were from peripheral retina (typically ∼30 degrees eccentricity based on ganglion cell dendritic field sizes).

Recordings and cell types

Recordings were made from ∼2 mm square pieces of retina, isolated from the choroid and pigment epithelium and mounted flat with the ganglion cells facing up in a recording chamber. During recording the retina was superfused with Ames solution heated to 32-34 °C. Putative ON and OFF parasol cells were identified from their large somata when viewed under infrared light and from their characteristic transient spike responses to light steps during cell-attached recordings. The identity of all recorded cells was confirmed at the end of recording from fluorescence images (see below). Only data from confirmed ON and OFF parasol cells is reported here. Light responses were stable over the 15-20 min experimental duration.

Currents were recorded using patch pipettes filled with an internal solution containing (in mM) 90 $CsCH_3SO_3$, 20 TEA-Cl, 10 HEPES, 10 Cs_2-EGTA, 10 sodium phosphocreatine, 2 QX-314, 4 Mg-ATP and 0.5 Mg-GTP; pH was adjusted to ∼7.2 with CsOH and osmolarity was ∼280 mOsm. Voltages were recorded using an internal containing (in mM) 125 K-Aspartate, 10 KCl, 10 HEPES, 5 NMG-HEDTA, 1 $MgCl_2$, 0.5 $CaCl_2$, 4 Mg-ATP, 0.5 Tris-GTP; pH was adjusted with NMG-OH. Internal solutions included 0.1 mM of either Alexa 488 or Alexa 555.

Parasol cells had an input resistance of 30-50 MΩ in recordings using the K^+ internal solution. Resting potentials were near -65 mV in the dark, and -55 mV in the presence of a mean light (see below). Series resistance during recordings was 8-12 MΩ, and was compensated 75%. All reported voltages were corrected for a -10 mV junction potential.

Light stimuli

Light stimuli were delivered from a light-emitting diode (LED) with a peak output at 513 nm. Light from the LED was focused on a 630 μm diameter spot centered between the two recorded cells. The mean light intensity used in all experiments produced ∼4000 effective photon absorptions per second in middle-wavelength sensitive (M) cones, assuming a collecting area of 0.37 μm^2 44. These light levels strongly emphasized cone-mediated responses, as indicated by a ∼3-fold difference in sensitivity to 513 nm vs 640 nm light (rod-mediated responses are ∼500 times more sensitive to 513 nm light). Modulated stimuli consisted of 50% contrast (SD/mean) Gaussian noise, bandwidth 0-60 Hz. The autocorrelation of this stimulus was considerably narrower than the cross-correlation functions in Figures 3e and f, and thus the dynamics of the stimulus did not limit the speed of the neural responses.

Imaging and analysis

Each recording ended with a series of images of the two cells obtained with a confocal microscope; each pixel represented a volume of 0.41 × 0.41 × 1 μm. Different channels of the microscope were used for the two cells.

Dendritic overlap was estimated from image stacks based on histograms of nearest-neighbor distances between the two cells. Images were thresholded to differentiate cellular processes from background. For several cell pairs adequate thresholding was not possible; these pairs

were omitted from the remainder of the analysis. The minimum distance (in three dimensions) between each nonzero pixel of one cell to a nonzero pixel of the other cell was then computed. Repeating this process for all nonzero pixels produced the distribution of nearest-neighbor distances (e.g. the cumulative distributions Fig. 1g). For all cell pairs retained in the analysis, nearest-neighbor distributions were insensitive to the 50% changes in the threshold chosen to identify cellular processes. Finally, overlap was estimated from the fraction of nearest-neighbor distances below a criterion distance - i.e. from the value of the cumulative nearest-neighbor distribution at the criterion distance (e.g. Fig. 1g). Supplementary Figure 1 online explores the dependence of overlap on the criterion distance.

Kinetics of correlated and uncorrelated input

To compare the kinetics of uncorrelated and correlated synaptic input, we corrected the autocorrelation function of a cell's total synaptic input for the contribution from correlated input. Thus we assumed that the total input *z* was the sum of uncorrelated input *x* and correlated input *y*:

$$Z = x + y.$$

The measured autocorrelation function for a cell's total synaptic input is then

$$C_{zz} = C_{xx} + C_{yy},$$

since *x* and *y* are independent - i.e. $C_{xy} = 0$. Thus the correlation function for a cell's uncorrelated input is

$$C_{xx} = C_{zz} - C_{yy}.$$

In practice, C_{xx} was estimated by subtracting the cross-correlation function for the input to two neighboring cells from a cell's autocorrelation function - i.e. by replacing C_{yy} by the cross-correlation between neighboring cells. This 'corrected' autocorrelation function is compared with the cross-correlation function between neighboring cells in the right panels of Figures 1c and d.

Model incorporating common input and reciprocal connections

Figure 6 is based on a model used to investigate the relative impact of common input and reciprocal connections to correlated activity between ON parasol cells. The low firing rate of OFF cells during constant light (e.g. Fig. 2b) precluded measuring their spike cross-correlation functions.

Parasol cells were modeled as isopotential spheres, and the relation between subthreshold currents and voltages was assumed to be passive. These simplifications permitted the model to be based entirely on parameters taken directly from experimental measurements. Thus the correlation structure of the common noise for a given cell pair was determined by fitting the cross-correlation function for voltage-clamp experiments (Fig. 1c). Common noise was

generated from a gaussian distribution with an autocorrelation function equal to the fit. The correlation structure for the independent inputs was similarly derived from the corrected autocorrelation function (Fig. 1c, right). The resulting correlated and uncorrelated inputs were weighted to reproduce the experimental fraction of the total input variance (0.3; see Fig. 1c) that was correlated; the two inputs were then summed together. Equating the modeled and measured spike autocorrelations provided values for the absolute refractory period (2.5 ms) as well as amplitude (4 mV) and decay time (8 ms) of the relative refractory period. Both absolute and relative refractory periods were implemented by elevating threshold. The average RC time constant for the current-to-voltage filter was measured from the ∼2 ms time constant of the voltage response to small steps of injected current. Finally, the threshold for spike generation was chosen as 4.5 mV to produce a typical ON parasol spontaneous firing rate of 20 Hz.

Reciprocal coupling was modeled as a 880 MΩ resistance between the two cells (compared to the membrane resistance of ∼30 MΩ). Subthreshold voltages and action potentials both affected the coupling currents. Experimentally, action potentials did not produce anomalously large coupling currents: eliciting an action potential in a current-clamped cell produced a ∼30 pA response in a neighboring voltage-clamped cell (not shown).

Statistics

T-tests were used to evaluate statistical significance. All error bars are standard errors.

Supplementary Material

Refer to Web version on PubMed Central for supplementary material.

Acknowledgments

We thank Jon Cafaro, EJ Chichilnisky, Gabe Murphy, Eric Shea-Brown and Jon Shlens for comments on the manuscript and for enlightening discussions, and Daniel Carleton, Eric Martinson and Paul Newman for excellent technical assistance. Support was provided by HHMI and NIH (EY-11850).

References

1. Usrey WM, Reid RC. Synchronous activity in the visual system. Annu Rev Physiol. 1999; 61:435–456. [PubMed: 10099696]
2. Averbeck BB, Latham PE, Pouget A. Neural correlations, population coding and computation. Nat Rev Neurosci. 2006; 7:358–366. [PubMed: 16760916]
3. Meister M, Lagnado L, Baylor DA. Concerted signaling by retinal ganglion cells. Science. 1995; 270:1207–1210. [PubMed: 7502047]
4. Dan Y, Alonso JM, Usrey WM, Reid RC. Coding of visual information by precisely correlated spikes in the lateral geniculate nucleus. Nat Neurosci. 1998; 1:501–507. [PubMed: 10196548]
5. Pillow JW, et al. Spatio-temporal correlations and visual signalling in a complete neuronal population. Nature. 2008
6. Romo R, Hernandez A, Zainos A, Salinas E. Correlated neuronal discharges that increase coding efficiency during perceptual discrimination. Neuron. 2003; 38:649–657. [PubMed: 12765615]
7. Zohary E, Shadlen MN, Newsome WT. Correlated neuronal discharge rate and its implications for psychophysical performance. Nature. 1994; 370:140–143. [PubMed: 8022482]
8. Petersen RS, Panzeri S, Diamond ME. Population coding of stimulus location in rat somatosensory cortex. Neuron. 2001; 32:503–514. [PubMed: 11709160]

9. Puchalla JL, Schneidman E, Harris RA, Berry MJ. Redundancy in the population code of the retina. Neuron. 2005; 46:493–504. [PubMed: 15882648]
10. Nirenberg S, Carcieri SM, Jacobs AL, Latham PE. Retinal ganglion cells act largely as independent encoders. Nature. 2001; 411:698–701. [PubMed: 11395773]
11. Mastronarde DN. Correlated firing of retinal ganglion cells. Trends Neurosci. 1989; 12:75–80. [PubMed: 2469215]
12. Meister M. Multineuronal codes in retinal signaling. Proc Natl Acad Sci USA. 1996; 93:609–614. [PubMed: 8570603]
13. Field GD, Chichilnisky EJ. Information processing in the primate retina: circuitry and coding. Annu Rev Neurosci. 2007; 30:1–30. [PubMed: 17335403]
14. Schnitzer MJ, Meister M. Multineuronal firing patterns in the signal from eye to brain. Neuron. 2003; 37:499–511. [PubMed: 12575956]
15. Schneidman E, Berry M. J. n. Segev R, Bialek W. Weak pairwise correlations imply strongly correlated network states in a neural population. Nature. 2006; 440:1007–1012. [PubMed: 16625187]
16. Shlens J, et al. The structure of multi-neuron firing patterns in primate retina. J Neurosci. 2006; 26:8254–8266. [PubMed: 16899720]
17. Vaney DI. Many diverse types of retinal neurons show tracer coupling when injected with biocytin or Neurobiotin. Neurosci Lett. 1991; 125:187–190. [PubMed: 1715532]
18. Dacey DM, Brace S. A coupled network for parasol but not midget ganglion cells in the primate retina. Vis Neurosci. 1992; 9:279–290. [PubMed: 1390387]
19. Mastronarde DN. Correlated firing of cat retinal ganglion cells. I. Spontaneously active inputs to X- and Y-cells. J Neurophysiol. 1983; 49:303–324. [PubMed: 6300340]
20. Mastronarde DN. Correlated firing of cat retinal ganglion cells. II. Responses of X- and Y-cells to single quantal events. J Neurophysiol. 1983; 49:325–349. [PubMed: 6300341]
21. Mastronarde DN. Interactions between ganglion cells in cat retina. J Neurophysiol. 1983; 49:350–365. [PubMed: 6300342]
22. Jacoby R, Stafford D, Kouyama N, Marshak D. Synaptic inputs to ON parasol ganglion cells in the primate retina. J Neurosci. 1996; 16:8041–8056. [PubMed: 8987830]
23. Brivanlou IH, Warland DK, Meister M. Mechanisms of concerted firing among retinal ganglion cells. Neuron. 1998; 20:527–539. [PubMed: 9539126]
24. DeVries SH. Correlated firing in rabbit retinal ganglion cells. J Neurophysiol. 1999; 81:908–920. [PubMed: 10036288]
25. Hu EH, Bloomfield SA. Gap junctional coupling underlies the short-latency spike synchrony of retinal alpha ganglion cells. J Neurosci. 2003; 23:6768–6777. [PubMed: 12890770]
26. Hidaka S, Akahori Y, Kurosawa Y. Dendrodendritic electrical synapses between mammalian retinal ganglion cells. J Neurosci. 2004; 24:10553–10567. [PubMed: 15548670]
27. Wassle H. Parallel processing in the mammalian retina. Nat Rev Neurosci. 2004; 5:747–757. [PubMed: 15378035]
28. Chichilnisky EJ, Baylor DA. Synchronized firing by ganglion cells in monkey retina. Neurosciences abstract. 1999
29. Boycott BB, Wassle H. Morphological Classification of Bipolar Cells of the Primate Retina. Eur J Neurosci. 1991; 3:1069–1088. [PubMed: 12106238]
30. de la Rocha J, Doiron B, Shea-Brown E, Josic K, Reyes A. Correlation between neural spike trains increases with firing rate. Nature. 2007; 448:802–806. [PubMed: 17700699]
31. Zaghloul KA, Boahen K, Demb JB. Different circuits for ON and OFF retinal ganglion cells cause different contrast sensitivities. J Neurosci. 2003; 23:2645–2654. [PubMed: 12684450]
32. Victor JD, Purpura KP. Nature and precision of temporal coding in visual cortex: a metric-space analysis. J Neurophysiol. 1996; 76:1310–1326. [PubMed: 8871238]
33. Murphy GJ, Rieke F. Network variability limits stimulus-evoked spike timing precision in retinal ganglion cells. Neuron. 2006; 52:511–524. [PubMed: 17088216]

34. Marshak DW, Yamada ES, Bordt AS, Perryman WC. Synaptic input to an ON parasol ganglion cell in the macaque retina: a serial section analysis. Vis Neurosci. 2002; 19:299–305. [PubMed: 12392179]
35. Bordt AS, Hoshi H, Yamada ES, Perryman-Stout WC, Marshak DW. Synaptic input to OFF parasol ganglion cells in macaque retina. J Comp Neurol. 2006; 498:46–57. [PubMed: 16856174]
36. Wassle H, Grunert U, Chun MH, Boycott BB. The rod pathway of the macaque monkey retina: identification of AII-amacrine cells with antibodies against calretinin. J Comp Neurol. 1995; 361:537–551. [PubMed: 8550898]
37. Hornstein EP, Verweij J, Schnapf JL. Electrical coupling between red and green cones in primate retina. Nat Neurosci. 2004; 7:745–750. [PubMed: 15208634]
38. Veruki ML, Hartveit E. AII (Rod) amacrine cells form a network of electrically coupled interneurons in the mammalian retina. Neuron. 2002; 33:935–946. [PubMed: 11906699]
39. Peichl L, Buhl EH, Boycott BB J Comp Neurol. Alpha ganglion cells in the rabbit retina. 1987; 263:25–41.
40. Dacey DM, Petersen MR. Dendritic field size and morphology of midget and parasol ganglion cells of the human retina. Proc Natl Acad Sci USA. 1992; 89:9666–9670. [PubMed: 1409680]
41. Chichilnisky EJ, Kalmar RS. Functional asymmetries in ON and OFF ganglion cells of primate retina. J Neurosci. 2002; 22:2737–2747. [PubMed: 11923439]
42. Schneidman E, Bialek W, Berry MJ. Synergy, redundancy, and independence in population codes. J Neurosci. 2003; 23:11539–11553. [PubMed: 14684857]
43. Dunn FA, Doan T, Sampath AP, Rieke F. Controlling the gain of rod-mediated signals in the Mammalian retina. J Neurosci. 2006; 26:3959–3970. [PubMed: 16611812]
44. Schnapf JL, Nunn BJ, Meister M, Baylor DA. Visual transduction in cones of the monkey Macaca fascicularis. J Physiol. 1990; 427:681–713. [PubMed: 2100987]

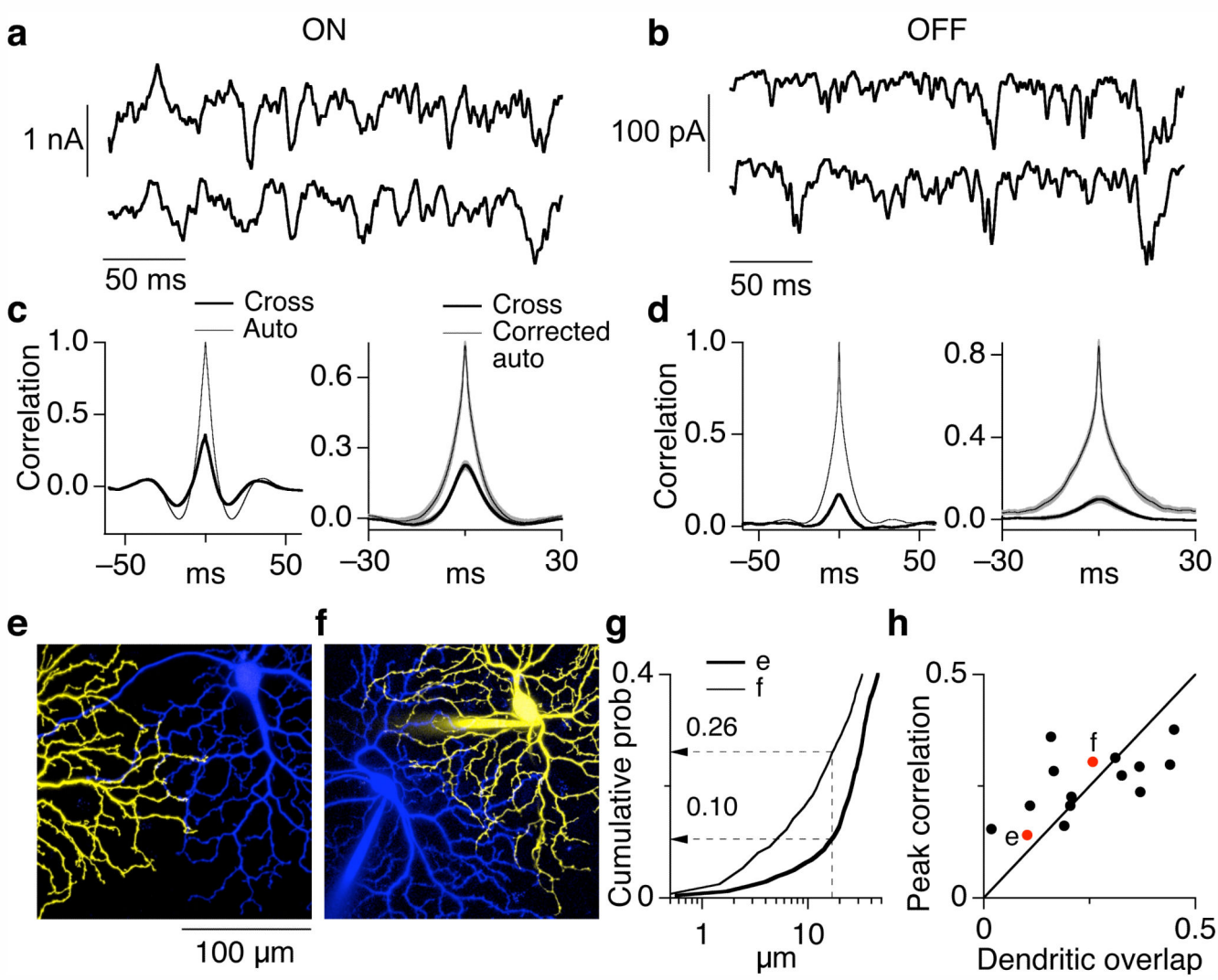

Figure 1.

Correlated variability in the synaptic inputs to neighboring ON and OFF parasol cells. (a, b) Simultaneously measured excitatory synaptic inputs to neighboring ON (a) and OFF (b) parasol cells at a holding potential of -70 mV. During recording the retina was exposed to a constant light producing ∼4,000 P*/cone/sec in M cones. (c, d) Quantification of common noise in synaptic inputs to neighboring parasol cells. The left panels compare the autocorrelation function (thin trace, average for two cells in pair) with the cross-correlation function (thick trace) for the cells in a and b. The right panels show the average cross-correlation functions and the corrected autocorrelation functions (mean ± SEM) across ON (c, n=16) and OFF (d, n=9) parasol pairs. 26 ± 2% (10 ± 2%) of the total variance was shared in ON (OFF) pairs. (e, f) Images of neighboring ON parasol cells with atypically little dendritic overlap (e) and typical dendritic overlap (f). The images shown are maximum point projections from a stack of images taken in different focal planes. (g) Cumulative distributions of nearest-neighbor dendritic distances for the cell pairs in e and f. (h) Dependence of correlation strength on dendritic overlap. Dendritic overlap was quantified

from cumulative distributions as in g; locations on one cell within 17 μm of a location on the other cell were defined as overlapping.

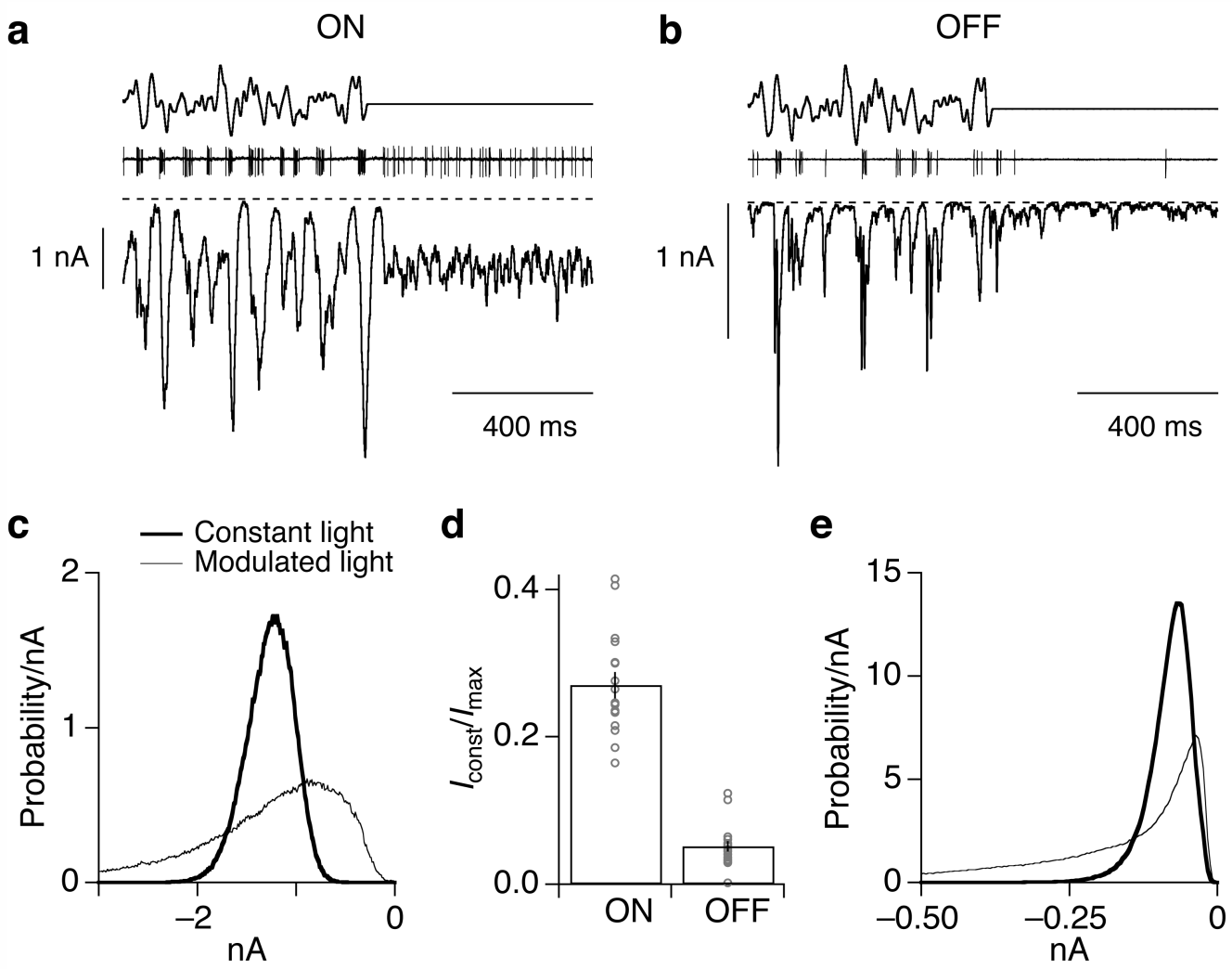

Figure 2.

OFF parasol cells receive less tonic excitatory input than ON parasol cells. (a, b) Stimulus (top), cell-attached recording of spike response (middle), and excitatory synaptic currents (bottom, holding potential -70 mV) for an ON (a) and an OFF (b) parasol cell. The mean light intensity produced ∼4,000 P*/cone/sec in M cones. Larger inward currents correspond to increased excitatory input. The dashed line denotes the current level without excitatory synaptic input, estimated from smallest current value observed during recording; this level was similar to the current remaining with glutamate, GABA and glycine receptors blocked (not shown). (c) Distribution of current amplitudes during modulated stimulus (thin trace) and constant light (thick trace) from the ON parasol cell in A. (d) Summary of tonic excitatory synaptic input to ON (n=18) and OFF (n=17) parasol cells during constant light. Points plot the mean current in constant light divided by the maximum current magnitude achieved during the modulated stimulus. (e) Distribution of current amplitudes for the OFF parasol in b.

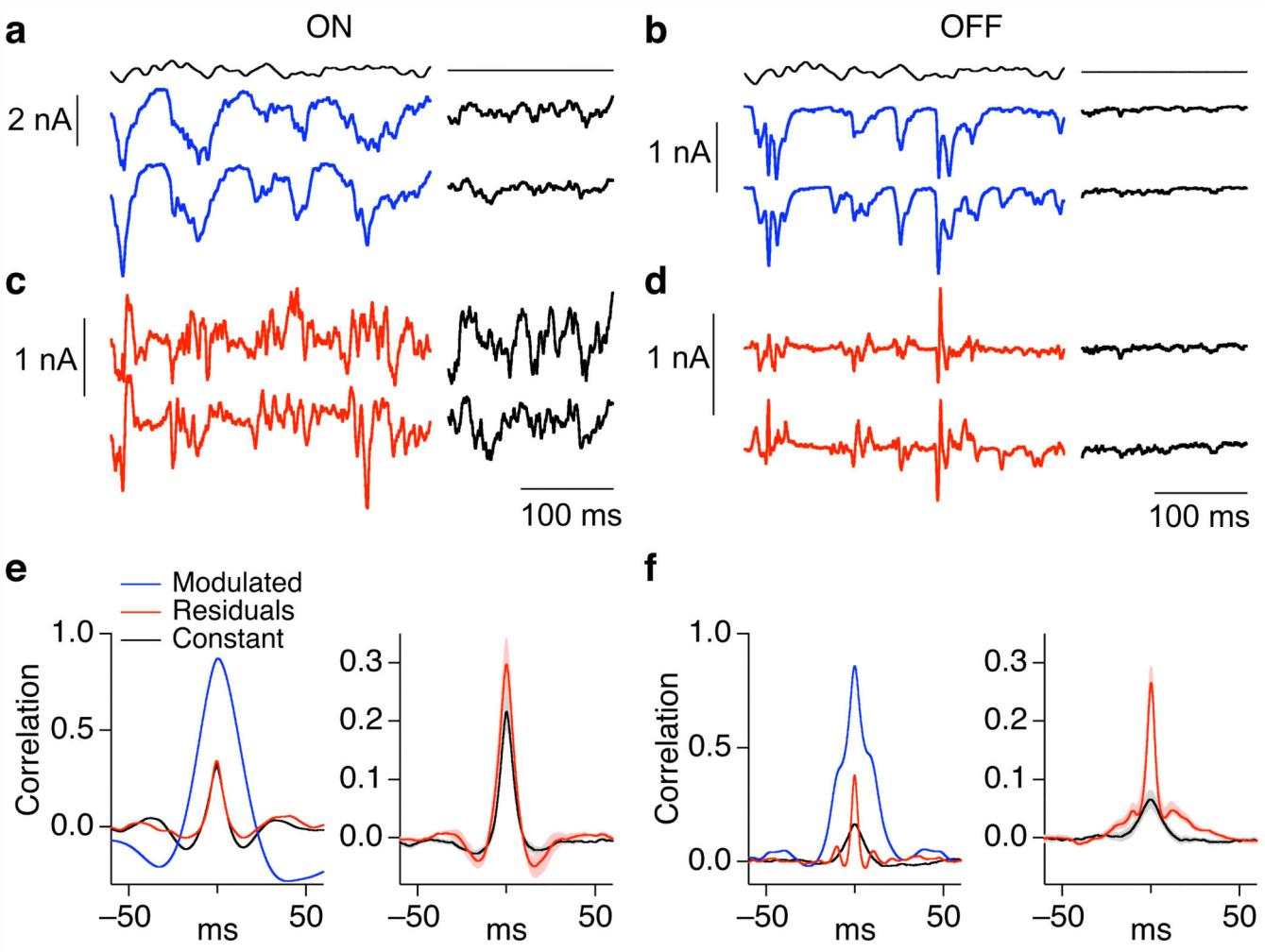

Figure 3.

Common noise in the excitatory synaptic inputs to OFF but not ON parasol cells depends on stimulus properties. (a, b) Simultaneously measured excitatory synaptic currents of neighboring ON (a) and OFF (b) parasol cells to a single presentation of a 50% contrast fluctuating stimulus (blue trace). During recording the retina was exposed to a constant light producing ~4,000 P*/cone/sec in M cones. Same cell pairs as Figure 1. (c, d) Residuals of responses from a and b, computed by subtracting the average response to 10 repetitions of the modulated stimulus from the individual responses. (e, f) Properties of correlated synaptic input for neighboring ON (e) and OFF (f) parasol cells. Left panels compare cross-correlation functions for total synaptic input during fluctuating light stimulus (blue trace), residuals during fluctuating light stimulus (red trace) and constant light (black trace). Right panels compare average cross-correlation functions (mean ± SEM, n=8 for ON pairs, n=9 for OFF pairs) for the residuals of the responses to modulated light and responses during constant light. The peak crosscorrelation during modulated light was 0.29 ± 0.04 in ON pairs (mean ± SEM) and 0.27 ± 0.03 in OFF pairs.

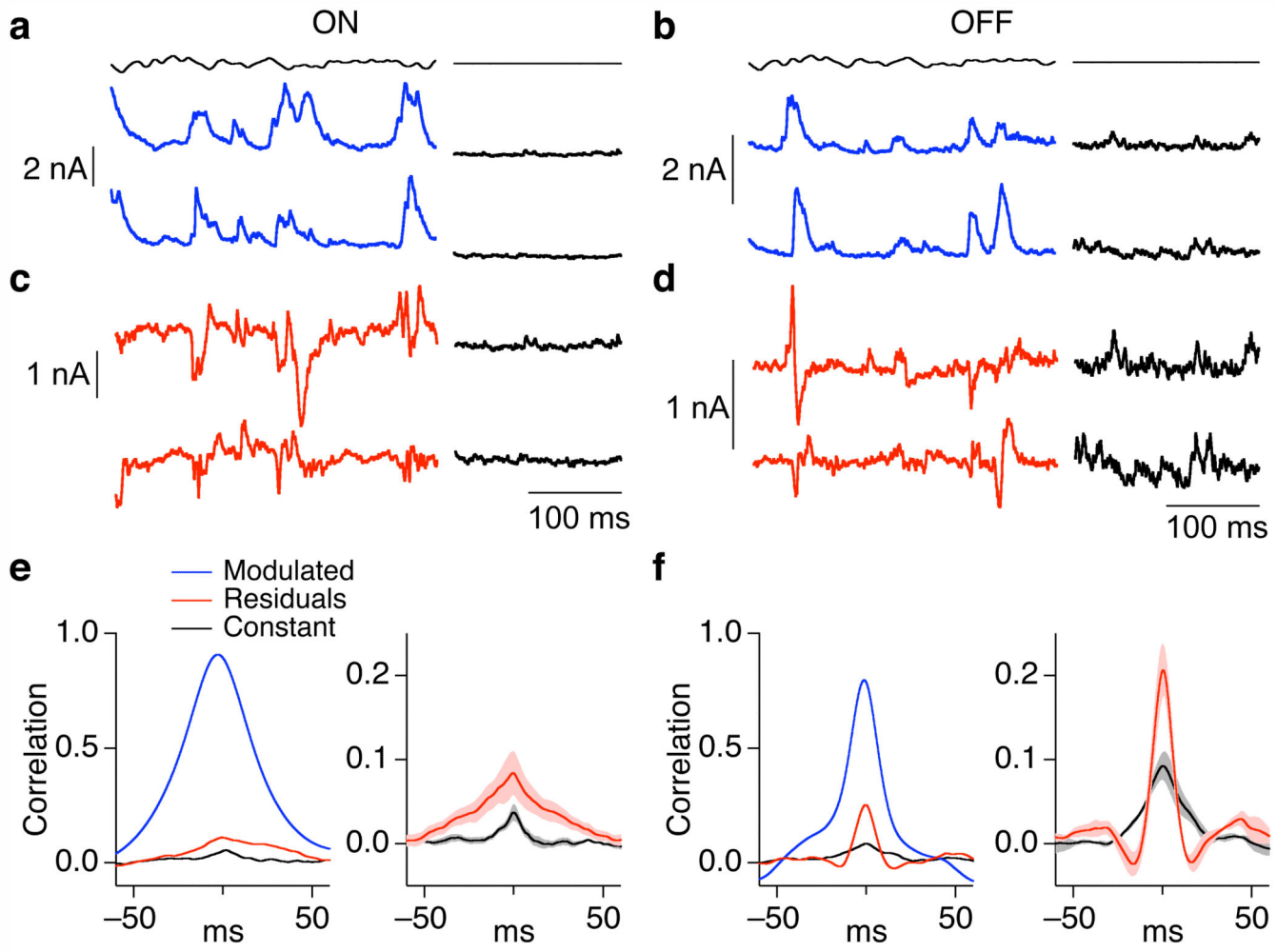

Figure 4.

Correlations in the inhibitory synaptic inputs to ON and OFF parasol cells. (a, b) Simultaneously measured inhibitory synaptic currents (holding potential ∼15 mV) of neighboring ON (a) and OFF (b) parasol cells to a single presentation of a 50% contrast fluctuating stimulus (blue trace). (c, d) Residuals of responses from a and b, computed by subtracting the average response to 10 repetitions of the modulated stimulus from the individual responses. (e, f) Properties of correlated synaptic input for neighboring ON (e) and OFF (f) parasol cells. Left panels compare cross-correlation functions for total synaptic input during fluctuating light stimulus (blue trace), residuals during fluctuating light stimulus (red trace) and constant light (black trace). Right panels compare average cross-correlation functions (mean ± SEM, n=7 for ON pairs, n=4 for OFF pairs) for the residuals of the responses to modulated light and responses during constant light.

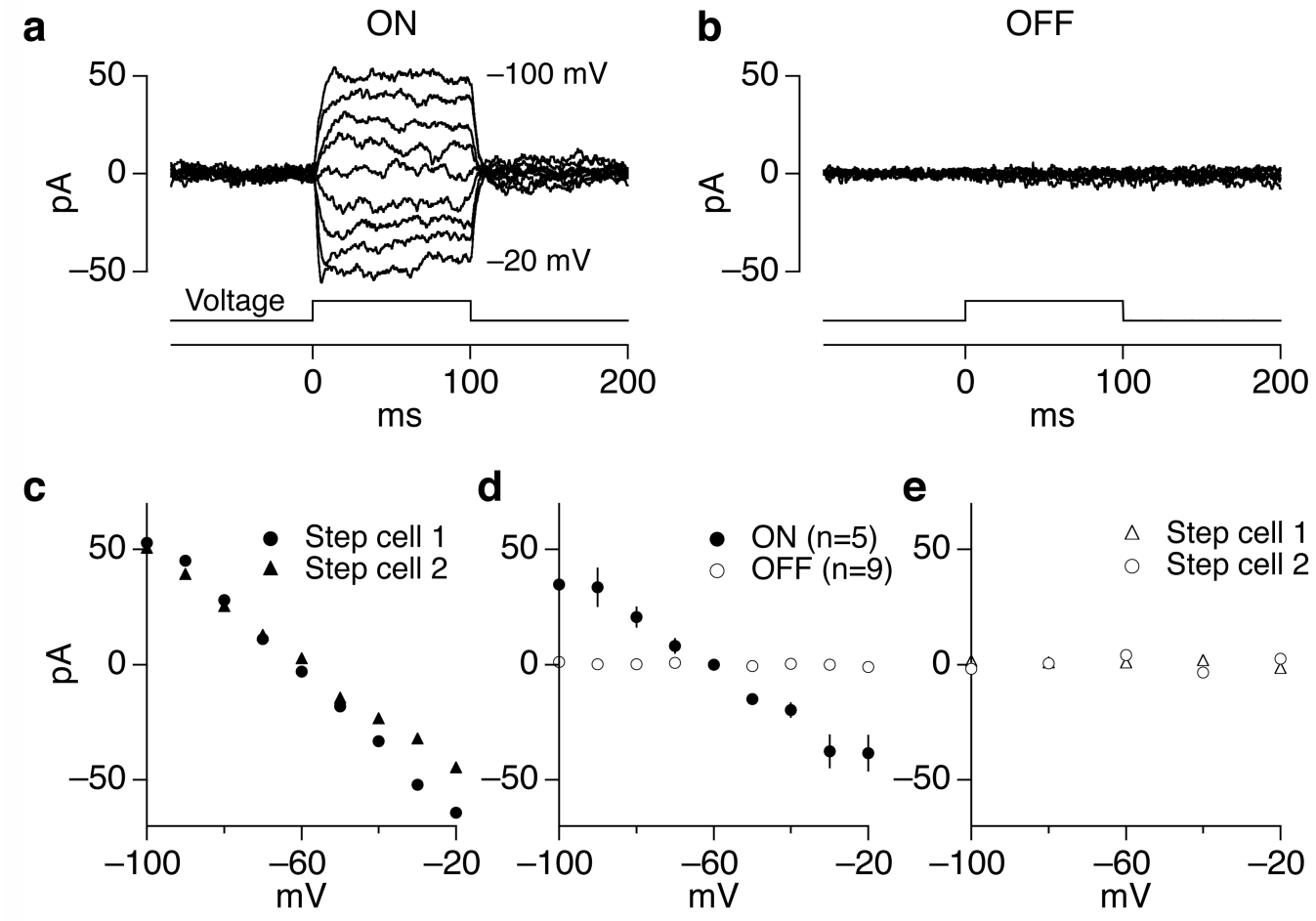

Figure 5.

ON but not OFF cells are effectively reciprocally coupled. (a, b) Coupling currents produced in an ON (a) or OFF (b) parasol cell by stepping the voltage of a neighboring ON or OFF cell. Voltage steps ranged from -100 to -20 mV in 10 (a) or 20 (b) mV increments. Holding potential of both cells was -60 mV. (c) Steady-state current measured during the second half of the step plotted against step voltage. Circles plot data from a, and triangles plot data when the coupling was measured in the opposite direction (i.e. when the voltage step was applied to the other cell). (d) Collected measurements of current-voltage relations for reciprocal connections. The rectification at large voltage differences likely was due to uncompensated series resistance, which would cause the actual voltage difference to be smaller than expected. The effective coupling resistance between ON parasol cells (the inverse of the slope of the current-voltage relation) was 880 ± 80 MOhm. The effective coupling resistance between OFF parasol pairs (resistance > 100 GOhm) was at least 100 times higher. (e) Current-voltage relation for OFF parasol pair from b. Activity of receptors mediating chemical synaptic transmission was suppressed with 10 μM NBQX, 20 μM APV and 10 μM strychnine.

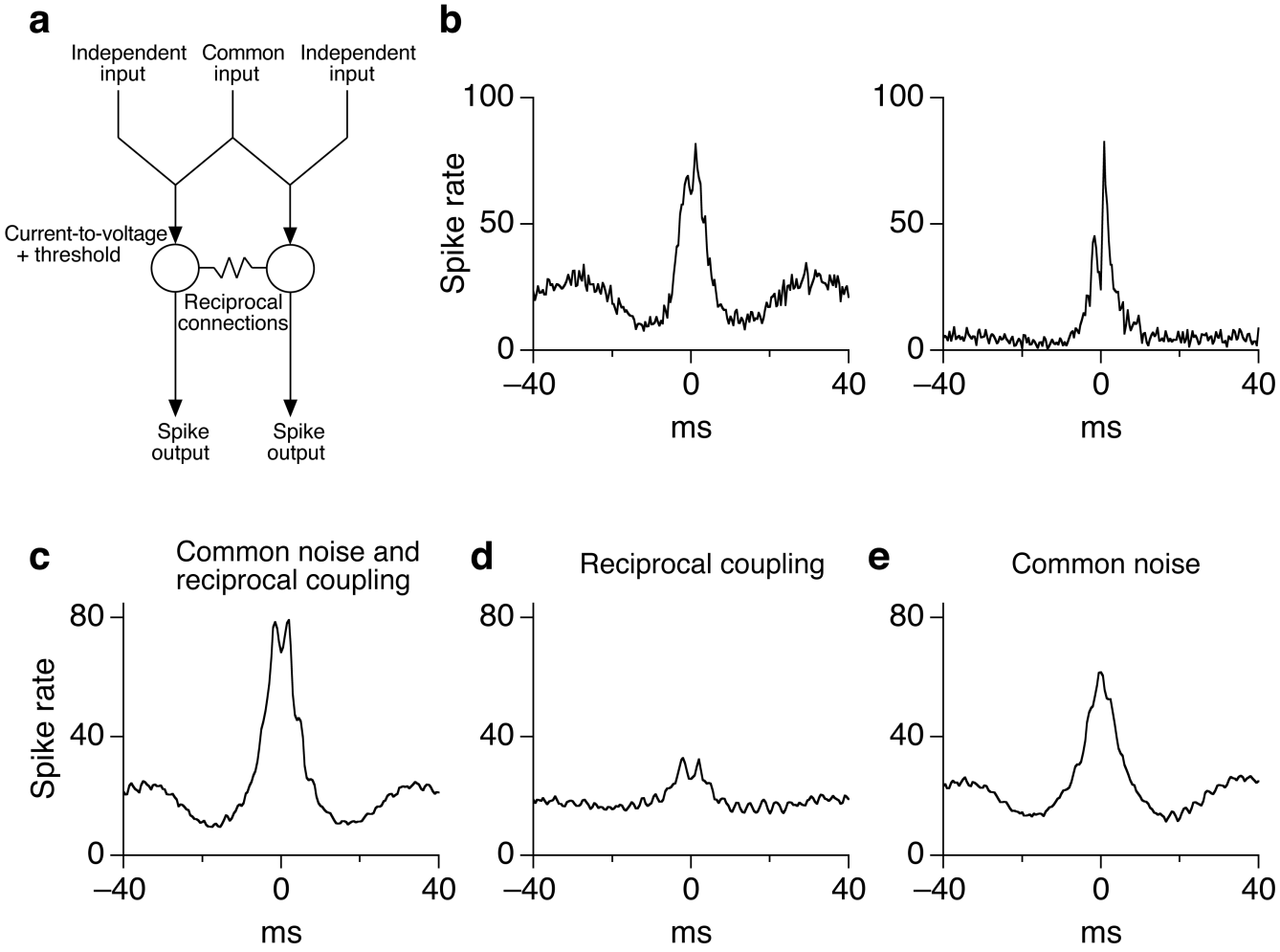

Figure 6.

Contributions of common noise and reciprocal connections to correlations between spike trains of ON parasol cells. (a) Schematic of model. (b) Two examples of measured cross-correlation functions for spike responses of neighboring ON parasol cells exposed to constant light. (c) Predicted cross-correlation function for ‘standard’ model with all parameters equal to those measured experimentally. (d) Predicted cross-correlation function with no common noise. (e) Predicted cross-correlation function with no reciprocal connections.

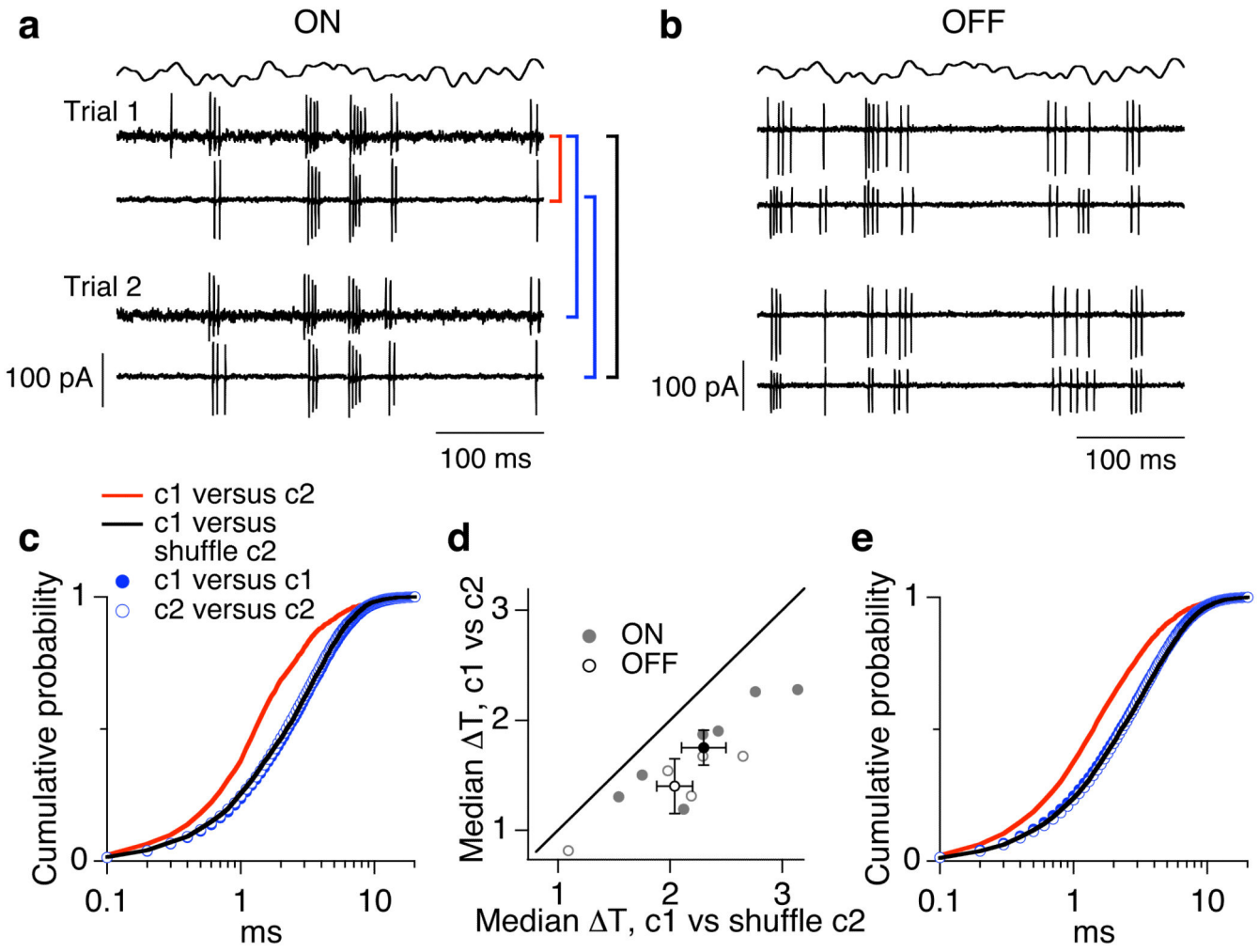

Figure 7.

Correlations affect temporal precision of ganglion cell spike responses. (a, b). Cell attached recordings of spike responses of neighboring ON (a) and OFF (b) parasol cells during modulated light stimulus. Responses to two repeats of the stimulus are shown for each cell pair. (c) Temporal precision of spike responses. Cumulative distributions of temporal offsets between spikes were calculated using the Victor distance metric to create spike pairs. Cumulative distributions are shown for responses of different cells recorded simultaneously (red) and nonsimultaneously (black) as well as for the same cell on different trials (blue and green circles). (d) Collected measurements of temporal precision for all pairs of ON (n=7) and OFF (n=5) parasol cells. (e) Temporal precision of spike responses for neighboring OFF parasol cells as in c.

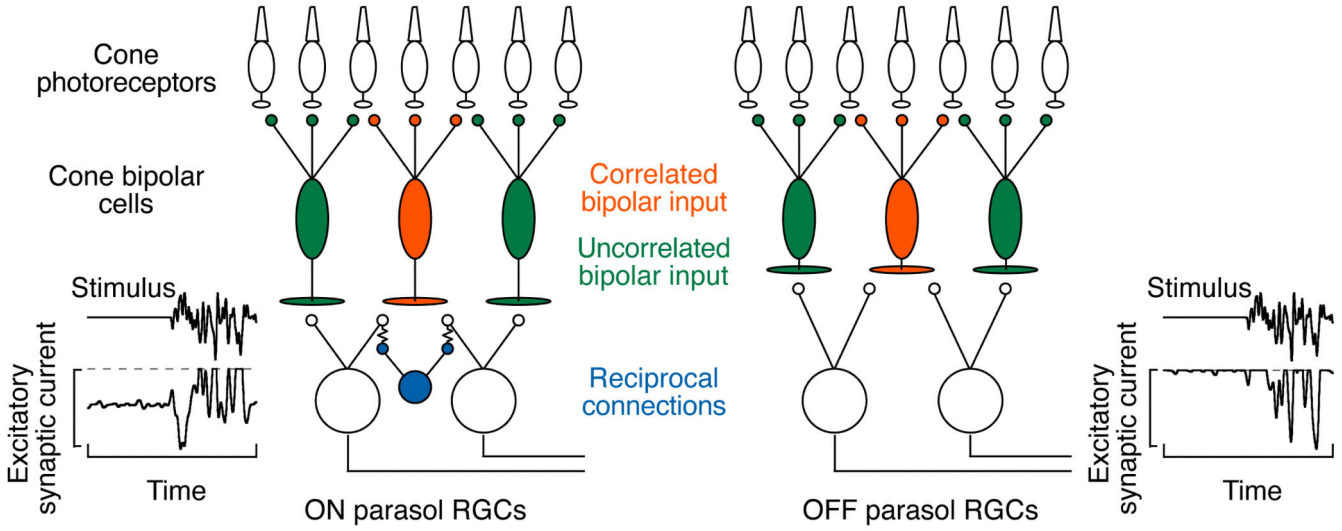

Figure 8.

Working model for mechanistic basis of correlated activity in neighboring ON and OFF parasol cells.